CHAPTER 4

Copper Oxide Nanostructures in Dye-sensitized Solar Cells

This chapter presents applications of mixed phase-copper oxide nanostructures, CuO-Cu_2O nanofibers and CuO-Cu_2O nanoparticles, as a thin layer on top of ZnO layer. The additional layer of copper oxide nanostructures is used to improve the ZnO DSSCs performance. The high carrier concentration and high absorption coefficient in visible light spectra of CuO and Cu_2O lead to applications in photovoltaic devices [26, 62, 117-119]. Moreover, they were expected to have better interaction in solar cells because of their unique physical properties and stable in nanostructure forms [120]. The power conversion efficiency was measured by using a solar simulator. The copper oxide layer can significantly improve the ZnO DSSCs efficiency by an increase of the charge carrier density. The enhancement can be explained in terms of effect of photovoltaic properties in the copper oxides layer in ZnO DSSCs.

4.1 Copper Oxide Nanofibers in ZnO based DSSCs

4.1.1 Device Fabrication

The mixed phases of CuO and Cu_2O nanofibers were synthesized by using pure copper powder as a precursor via microwave heating under normal atmosphere for a few minutes as discussed in the chapter 2. Then, different nanofibers masses (1.14, 2.28, 3.42, 4.56, and 5.70 mg) were mixed with an equal mass of polyethylene glycol (PEG) in 4 mL of ethanol and stirred for 1 h. The nanofiber paste was then coated on a 1 cm^2 ZnO layer. Therefore, the different copper oxide layer surface densities were 1.14, 2.28, 3.42, 4.56, and 5.70 mg/cm^2.

A ZnO layer was prepared from ZnO nanopowders, ~30 nm in diameter coated on FTO conduction glass. The prepared photoelectrode was then heated at 400^0C for 1 h before soaking it into N719 solution (0.5 mM, Dyesol)

47

for 1 h. Counter electrodes were prepared by coating Pt solution, composed of acetone (1 cm^3) and hydrogen hexachloroplatinate (IV) hydrate (0.012 g), on FTO glass. Next, the FTO glass was heated at 400°C for 1 h. Finally, the ZnO DSSC was assembled by sealing the photoelectrode and counter electrode in hot double layers of plastic paraffin film ($\sim$50 μm thickness). The gap between electrodes was filled with an electrolyte solution (0.2 M of LiI, 0.02 M of I$_2$, 0.5 M of DMP II, 0.5 M of TBP and 10 mL of Acetonitrile). The DSSC structures of this work were sketched as shown in Figure.4.1

The following instruments were used to characterize the ZnO DSSCs: scanning electron microscope (SEM); energy dispersive spectroscope (EDS); photocurrent density-voltage measurement (*J-V*); electrochemical impedance spectroscope (EIS); and ultraviolet–visible (UV–vis) spectrometer.

4.1.2 Effects of Copper Oxide Nanofibers in DSSCs

After microwave heating, mixed phases of CuO and Cu$_2$O nanofibers were obtained as shown by XRD patterns in Figure 4.2. CuO exhibited a peak at (002). Conversely, Cu$_2$O showed sharp peaks at (111), (200) and (220). The ratio of CuO: Cu$_2$O was about 13.60 : 86.40%.
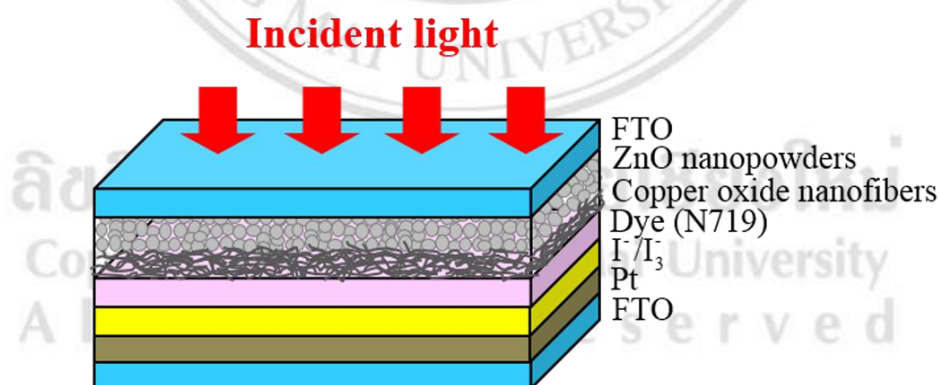

Figure 4.1 Schematic diagram of ZnO DSSC structures with copper oxide nanofibers as a double layer in photoelectrode.
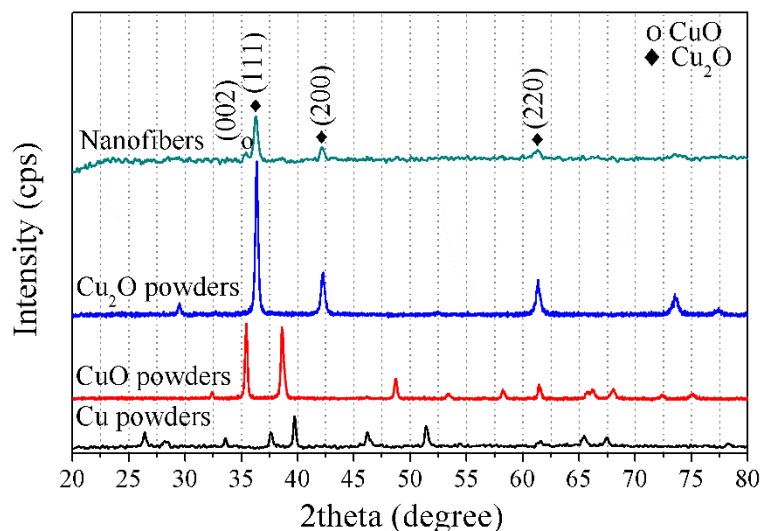
Figure 4.2 XRD patterns of copper oxide nanofibers comparing to Cu powders, CuO and Cu_2O powders.
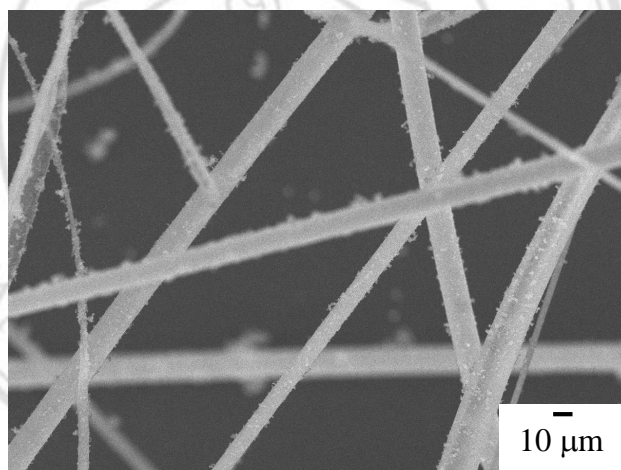

Figure 4.3 SEM image of copper oxide nanofibers**.**

The morphology of the copper nanofibers showed circular cylindrical shape and smooth surface with average diameters between 290-400 nm as shown in Figure 4.3.

The ZnO nanopowders were screened on FTO glass and coated with copper oxide nanofibers as shown in Figure 4.4. The SEM image in Figure 4.4 (a) shows cross-sections of the ZnO/mixed-phase copper oxide nanofiber layer (3.42 mg/ cm^2) on FTO glass. The thickness of ZnO layer was about 14 μm. The surface of the ZnO and copper oxide layer (3.42 mg/ cm^2) is shown in Figure 4.4 (b) and (c).
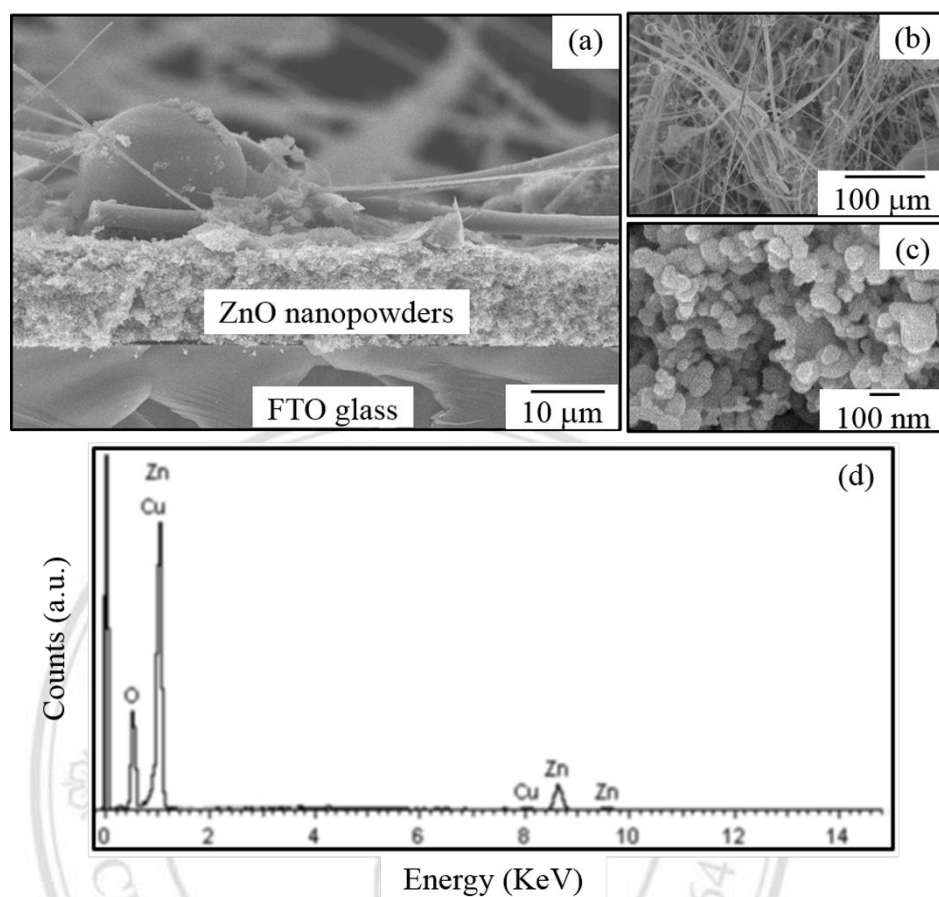
49

Figure 4.4 SEM images of (a) cross-section of ZnO nanopowders / copper oxide nanofibers (3.42 mg/cm²), (b) and (c) surface of ZnO nanopowders and copper oxide nanofibers (3.42 mg/cm²), and (d) EDS spectrum of ZnO/copper oxide nanofibers (3.42 mg/cm²).

The chemical composition of the photoelectrode consisting of two layers (ZnO/copper oxide layer) was investigated using EDS. The EDS spectrum of the ZnO/copper oxide layer (3.42 mg/ cm²) shows Zn, O, and Cu signals as shown in Figure 4.4 (d).

The *J-V* characteristics of these devices are shown in Figure 4.5. The best J_{SC} (short circuit current density) observed at 3.42 mg/ cm² was 6.93 mA/cm², which was 26% greater than that of the pure ZnO DSSCs.
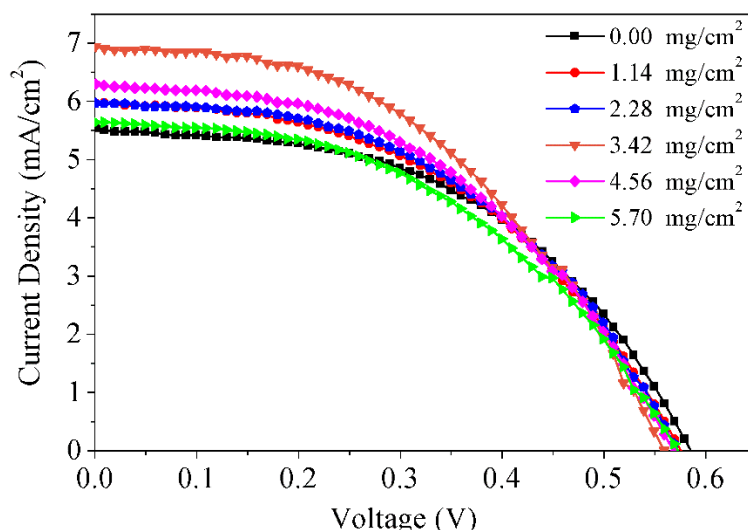
Figure 4.5 $J-V$ characteristics of ZnO DSSCs with different surface densities of copper oxide in photoelectrodes.

Figure 4.6 shows power conversion efficiencies (η) of the ZnO DSSCs prepared with different surface densities of the mixed-phase copper oxide nanofibers. The ZnO DSSCs without a copper oxide layer exhibited a power conversion efficiency of 1.62%. After nanofiber coating, the efficiencies of the ZnO DSSCs steadily increased as the surface density of copper oxides increased and the highest efficiency of 1.87% was obtained at a density of 3.42 mg/cm^2. Beyond the peak efficiency, it declined steadily to 1.74% and 1.55% at densities of 4.56 and 5.70 mg/cm^2, respectively. The significant increase in the J_{SC} indicated that the mixed-phase copper oxide nanofibers, as a double layer, are able to improve photocurrent in ZnO DSSCs. The results corresponded to amounts of dye loading in the photoanode as shown in Table 4.1. The adsorbed moles were calculated by using absorbance spectra, the extinction coefficient of dye and the Lambert Beer law [121, 122]. The copper oxide layer with a surface density of 3.42 mg/cm^2 can adsorb a maximum dye of 5.12×10^{-6} mol/cm^2. This observation allows us to state that the large internal surface area for dye adsorption of copper oxide nanofibers played a key role to adsorb more incident light in almost wavelength range of UV-visible light and improved charge carrier density. The photovoltaic parameters of these devices are summarized in Table 4.1.
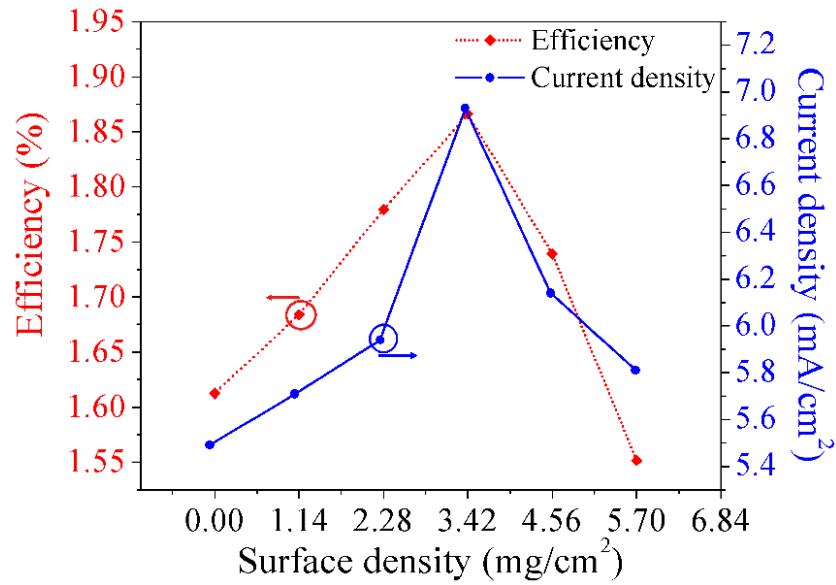
Figure 4.6 Power conversion efficiency (left) and current density (right) of ZnO DSSCs with copper oxide layer as a function of surface densities of copper oxide nanofibers layer in photoelectrodes.

Table 4.1 Summary of ZnO DSSCs parameters including dye loading, short circuit current density (J_{SC}), open circuit voltage (V_{OC}), fill factor (FF) and power conversion efficiency.

SDCL[*] (mg/cm^2)	CCF[**] (mM/L)	Dye loading (10^{-6}mol/cm^2)	J_{SC} (mA/cm^2)	V_{OC} (V)	FF	η (%)
0.00	0	2.10	5.49	0.57	0.44	1.62
1.14	2	3.69	5.71	0.57	0.49	1.68
2.28	4	4.26	5.94	0.57	0.48	1.78
3.42	6	5.12	6.93	0.56	0.48	1.87
4.56	8	4.92	6.14	0.56	0.48	1.73
5.70	10	3.86	5.81	0.57	0.44	1.55

[*] Surface densities of copper oxide layer

[**] Concencration of nanofibers

Efficiency (η) of the ZnO DSSCs can be calculated from J_{SC}, open circuit voltage (V_{OC}), fill factor (FF) and the intensity of the incident light (P_{in}) using the following equation : [123]

$$\eta = \frac{V_{OC}\, J_{SC}\, FF}{P_{in}}.$$ (4.1)

The copper oxide layer has a negligible effect on the V_{OC} and FF. The efficiency enhancement was mainly caused by increase in the J_{SC}. The highest value of the J_{SC} corresponded to a maximum efficiency of 1.87%, as shown in Table 4.1. This was to be expected due to the optical properties of copper oxide nanofibers. Figure 4.7 shows the UV-vis absorption spectra of ZnO/copper oxide nanofibers and pure ZnO layer with 1 h of dye loading. The pure ZnO layer exhibited an intrinsic absorption with intensity below 380 nm due to its band gap absorption. Conversely, ZnO/copper oxide nanofibers layer showed absorption in the whole wavelength region of UV-visible light and exhibited the highest absorption in the range of 420-600 nm. The increased current density of mixed-phase copper nanofiber layer is therefore due to their wider photon absorption range.
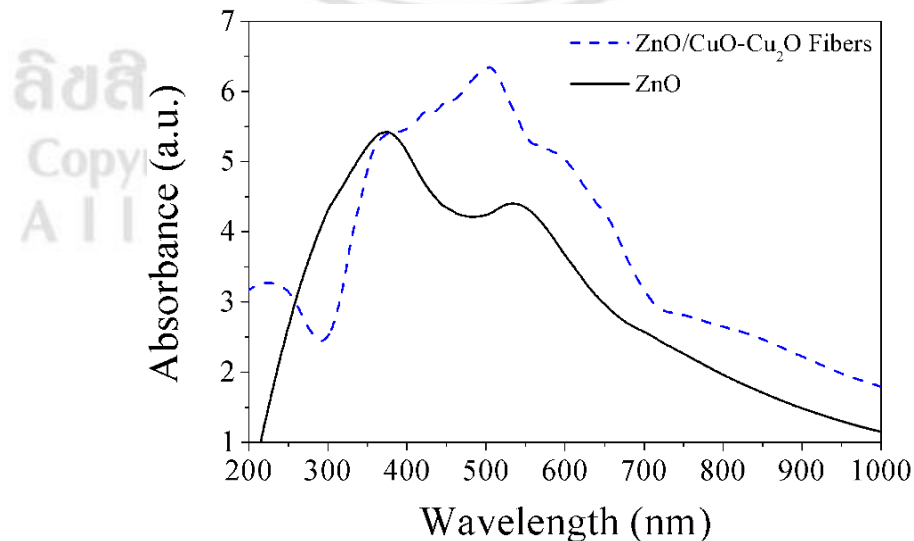

Figure 4.7 UV-vis absorption spectra of N179 dye-coated copper oxide nanofibers (3.42 mg/cm^2) on ZnO comparing to pure ZnO layer.
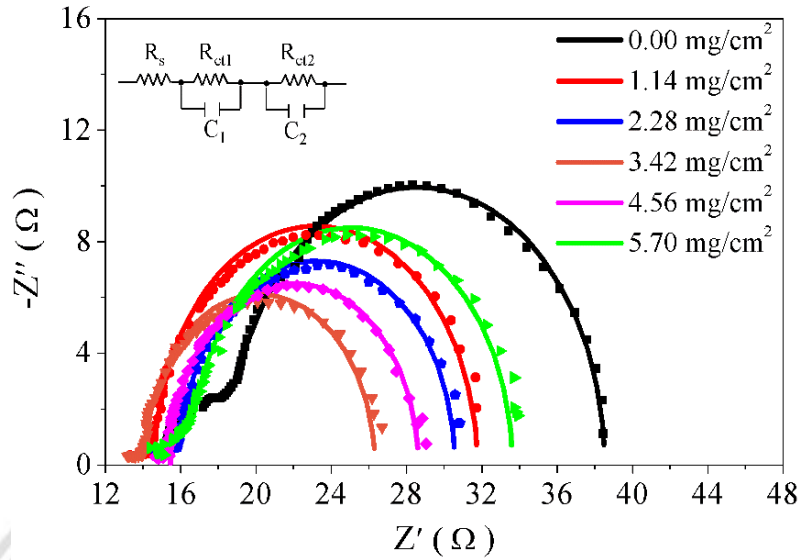
53

Figure 4.8 EIS spectra of ZnO DSSCs with different surface densities of copper oxide nanofibers layer. Experimental data are represented by solid symbols and solid lines correspond to fitted data.

Furthermore, EIS analysis displayed effect of the copper oxides on electron recombination. EIS spectra of the ZnO DSSCs with different surface densities of nanofibers were shown in Figure 4.8.

The EIS analysis was operated with an AC amplitude of 20 mV at 100 mW/cm² from 1 to 10,000 Hz under solar light. The EIS data were fitted using an equivalent circuit, as shown in the inset of Figure 4.8, via Z-View software. The extracted electrochemical parameters, shunt resistance (R_{sh}), series resistance (R_s), charge transfer resistance ($R_{ct(total)} = R_{ct1} + R_{ct2}$), and electron lifetime (τ) are summarized in Table 4.2. Note that R_{sh} represents the manufacturing defects that became an alternate path for the flow of current. The R_{sh} was calculated from the inverse slope of *J-V* curve at the J_{SC}. The electron lifetime τ is related to electron recombination in DSSCs by means of a characteristic time constant, which can be estimated from the maximum angular frequency (ω_{max}) of the impedance, as follows: [124, 125]

Table 4.2 Summary of electrochemical parameters of the ZnO DSSCs at different copper oxide concentrations including shunt resistance (R_{sh}), series resistance (R_s), charge transfer resistance (R_{ct}), and electron lifetime (τ).

SDCF[*] (mg/cm^2)	CCF[**] (mM/L)	R_{sh} (Ω)	R_s (Ω)	R_{ct} (Ω)	τ (ms)
0.00	0	884.72	36.33	19.74	4.68
1.14	2	831.48	37.53	17.12	4.19
2.28	4	956.57	33.78	14.89	4.97
3.42	6	1,095.19	30.96	13.42	5.31
4.56	8	678.02	34.35	15.47	4.97
5.70	10	654.26	41.55	16.93	4.68

[*] Surface densities of CuO-Cu$_2$O nanofiber layer

[**] Concencration of CuO-Cu$_2$O nanofibers layer

$$\tau = \frac{1}{\omega_{max}} = \frac{1}{2\pi f_{max}}, \tag{4.2}$$

where f_{max} is the maximum frequency of the middle frequency peak.

The enhancement in shunt resistance R_{sh} and the reduction in series resistance R_s contributed to improvement in cell efficiency at the maximum value of 1.87% for 3.42 mg/cm^2. It was obvious that the highest value of the R_{sh} was 1,095.19 Ω at 3.42 mg/cm^2. This implied that the mixed-phase nanofibers had an effect on the decrease of current leakage.

The R_s specified the transport resistance of the FTO and $R_{ct(total)}$ pointed to charge transfer resistance through the photoelectrode/electrolyte. At density of 3.42 mg/cm^2 both resistances (R_s and $R_{ct(total)}$) showed the smallest values of 30.96 and 13.42 Ω and the longest electron lifetime (τ) at 5.31 ms.

In the case of p-type material such as the copper oxide nanofibers, the recombination rate (R) per unit volume per second through a single level defect or trap in high injection, can be written as : [126]

$$R \approx \frac{p}{\tau_p + \tau},$$ (4.3)

where p is the number of holes and τ_p is the hole lifetime. Thus, if the carrier lifetime (τ_p, τ) increases, the recombination rate will be low.

In contrast, the ZnO DSSCs at densities of 4.56 and 5.70 mg/cm^2 showed lower efficiency. It was noticed that the increased density of the nanofibers resulted in overlapping branches and surfaces resulting in less surface area for dye adsorption than that of the separated branches (concentration < 4.56 mg/cm^2). Thus, the ZnO DSSCs with nanofibers coating at 4.56 and 5.70 mg/cm^2 could absorb less dye and caused a decrease of electron injection. Moreover, a higher ZnO DSSC efficiency could also be confirmed by the electron lifetime (τ) as shown in Table 4.2. It could be said that the electron lifetime was longer with the optimum fiber density. It was probably due to higher crystalline fibers so electrons can be injected faster than a random crystalline network resulting in the rate increase of electron [24, 127]. The ZnO DSSCs with copper oxide nanofibers as a coating layer clearly exhibited that significant increase of light absorption improved the J_{SC} and the electron lifetime (τ) leading to suppression of electron recombination and enhancement of DSSC efficiency. It can be noted that an optimized surface density of copper oxide nanofiber can be used as a coating layer in photo electrodes to increase charge carriers, suppress recombination and improve the conversion efficiency of ZnO DSSCs.

4.2 Copper Oxide Nanoparticles in ZnO based DSSCs

4.2.1 Device Fabrication

The composite layer in photoelectrode, ZnO/CuO-Cu$_2$O, was prepared. The copper oxide nanoparticles were dissolved in polyethylene glycol (PEG) and ethanol solution with various weights of the nanoparticles obtaining different concentrations of about 2, 4, 6 and 8 mM (using molar mass of Cu$_2$O as a reference because the ratio is highest up to 86.40%). The ratio of the nanoparticles, PEG and ethanol was 1: 1 by weight: 1 mL, respectively. Then, the mixed solution was stirred for 1 h and screened on a ZnO layer, area 1 cm^2 (preparation from ZnO nanopowders, Nano Materials Technology Co. Ltd., diameter ~30 nm, coated on a FTO glass). The prepared photoelectrode was heated at 400^{0}C for 1 h before soaking in N719 for 1 h (0.5 mM, Dyesol). While, pure CuO (Sigma Aldrich, diameter < 50 nm) layer at 6 mM was also prepared as a reference. In preparation for counterelectrode, Pt solution containing acetone 1 cm^3 and hydrogen hexachloroplatinate (IV) hydrate 0.012 g was screened on a FTO glass and heated at 550^{0}C for 1 h. Finally, the DSSC was assembled by sealing the photoelectrode and counterelectrode via a hot double layer of parafilm (~50 μm thickness). The gap between electrodes was filled with electrolyte solution before the DSSC measurement.

The photovoltage (V_{OC}), photocurrent density (J_{SC}) and power conversion efficiency (η) were measured under a solar simulator at 100 mW/cm^2 of radiant power with AM 1.5 filter. The electrical properties were confirmed by electrochemical impedance spectroscopy (EIS) in the frequency range of 1-10,000 Hz. In addition, the optical properties were confirmed by ultraviolet–visible (UV–vis) spectrometer.

4.2.2 Effects of Copper Oxide Nanoparticles in DSSCs

A perspective of multilayer in DSSC was shown in Figure 4.9 (a). Figure 4.9 (b) showed cross-section SEM images of ZnO/CuO-Cu$_2$O layer (6 mM) on FTO glass. The thickness of CuO-Cu$_2$O layer was seen approximately
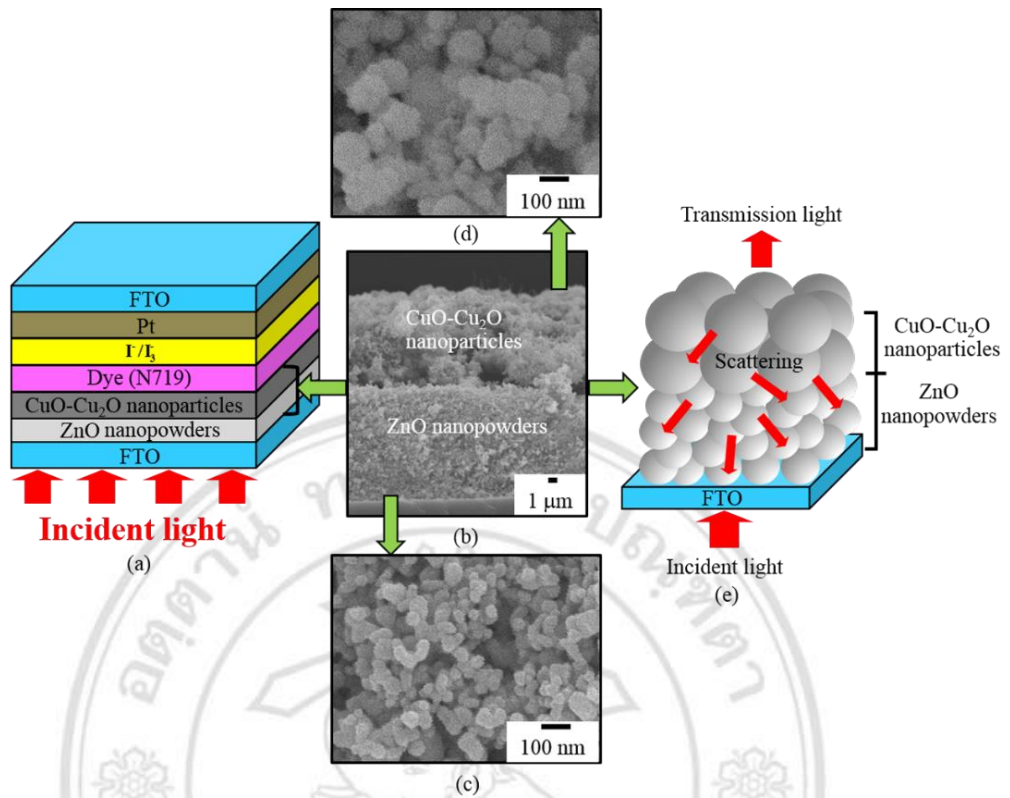
Figure 4.9 (a) Schematic diagram of ZnO DSSC structures, (b) cross-section SEM images of ZnO/CuO-Cu₂O at 6 mM, (c) and (d) FE-SEM images of ZnO nanopowders and CuO-Cu₂O nanoparticles, and (e) schematic illustration of light scattering of ZnO/CuO-Cu₂O nanoparticles.

6.9 μm. While, the thickness of ZnO layer was about 11.3 μm. The average diameter of ZnO nanopowders and CuO-Cu₂O nanoparticles were about 30 nm and 100 nm as shown in Figure 4.9(c) and 4.9 (d), respectively.

Figure 4.10 showed J - V characteristic graphs of ZnO DSSCs with different CuO-Cu₂O concentrations at 0, 2, 4, 6 and 8 mM. It was clearly observed that the DSSC exhibited the highest current density of 7.33 mA/cm² at 6 mM. This was consistent with the highest power conversion efficiency (η) of 2.31% as shown in the Figure 4.11.
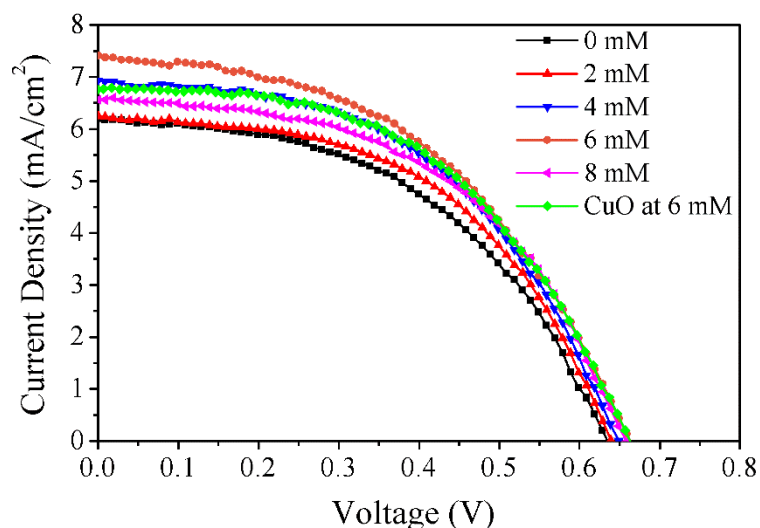
Figure 4.10 J -V characteristics of ZnO DSSCs with various concentrations of CuO-Cu₂O particle as additional layer in photoelectrodes.
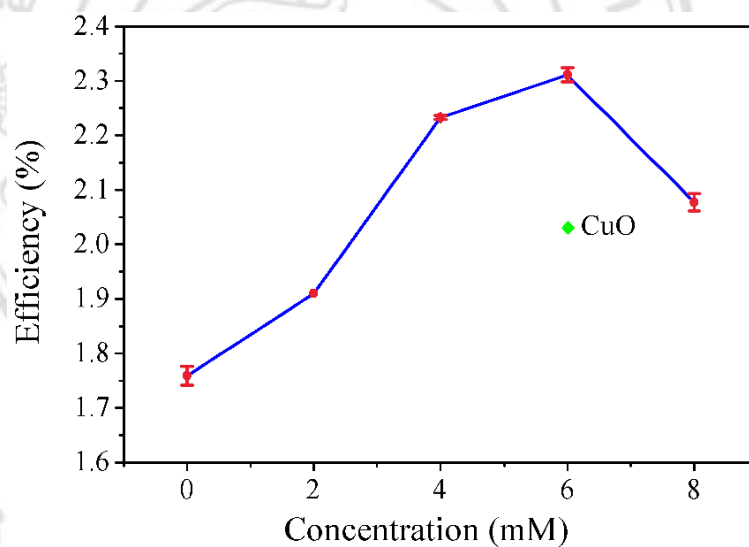

Figure 4.11 Power conversion efficiency of ZnO DSSCs with various concentrations of CuO-Cu₂O particle as additional layer in photoelectrodes. The efficiency of DSSC with pure CuO powders (6 mM) was compared.

The photovoltaic parameters of the DSSCs were summarized in Table 4.3. Importantly, the current density (J_{SC}) of the DSSC with the CuO-Cu₂O nanoparticles was higher by more than 7.30% compared to the DSSC with pure CuO. The results corresponded to amounts of dye loading in the photoanode. The adsorbed moles were calculated by using absorbance spectra, the extinction coefficient of dye and the Lambert Beer law [121, 122].

Table 4.3 Summary of ZnO DSSCs parameters with CuO-Cu$_2$O nanoparticle layer.

CCN* (mM)	Dye loading (10^{-6} mol/cm^2)	J_{SC} (mA/cm^2)	V_{OC} (V)	FF	η (%)
0	2.10	6.17	0.63	0.49	1.76
2	2.78	6.25	0.64	0.51	1.91
4	3.47	6.93	0.65	0.50	2.23
6	4.26	7.33	0.65	0.48	2.31
6**	3.70	6.77	0.66	0.51	2.03
8	3.24	6.56	0.65	0.51	2.08

*Concencration of CuO-Cu$_2$O nanoparticle layer

** Pure CuO as a reference

The copper oxide layer with a concentration of 6 mM can adsorb a maximum dye of 4.26×10^{-6} mol/cm^2. It is believed that the highest efficiency could be responsible for the better of photovoltaic properties and light scattering.

Next, the DSSCs will be explained in terms of electrical properties from electrochemical impedance spectroscopy (EIS). Figure 4.12 showed EIS spectra of ZnO DSSCs with different concentrations of CuO-Cu$_2$O nanoparticle layer with forward bias voltage.
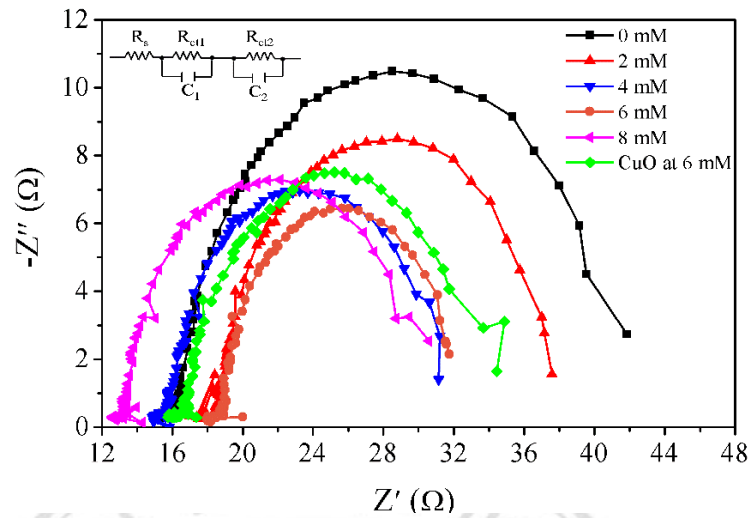
Figure 4.12 Impedance spectra of ZnO DSSCs with different concentrations of CuO-Cu$_2$O layer and pure CuO layer at 6 mM, at forward bias voltage.

The EIS analysis was operated with AC amplitude of 20 mV at 100 mW/cm^2 from 1 - 10,000 Hz under solar light. The EIS data was then plotted using ZView software to determine the electrochemical parameters; series resistance (R_s), shunt resistance (R_{sh}), charge transfer resistance (R_{ct}), and electron lifetime (τ) as shown in Table 4.4.

Table 4.4 Summary of electrochemical parameters of the ZnO DSSCs at different copper oxide concentrations including shunt resistance (R_{sh}), series resistance (R_s), charge transfer resistance (R_{ct}), and electron lifetime (τ).

CCN[*] (mM)	R_s (Ω)	R_{sh} (Ω)	R_{ct} (Ω)	τ (ms)
0	34.47	650.08	22.70	4.68
2	33.02	797.41	17.79	4.97
4	32.53	605.22	14.86	4.19
6	33.29	605.29	13.26	4.97
6[**]	34.71	1,154.02	15.95	4.97
8	31.16	927.16	15.68	4.42

[*]Concencration of CuO-Cu$_2$O nanoparticle layer

[**] Pure CuO as a reference

R_s was the transport resistance of FTO glass. The results showed that R_s and τ of the CuO-Cu$_2$O nanoparticle layers with various concentrations on ZnO DSSCs gave no significant difference.

According to the Bode phase plots, τ within photoelectrodes can be estimated from the maximum angular frequency (ω_{max}) as follows [128]

$$\tau = \frac{1}{\omega_{max}} = \frac{1}{2\pi f_{max}}, \qquad (4.4)$$

where f_{max} is the maximum frequency from impedance semicircle at the middle frequency peak. Moreover, τ can be deduced from the derivative of the open circuit voltage (V_{OC}) as follows: [129, 130]

$$\tau = -\frac{k_B T}{e} \left(\frac{dV_{OC}}{dt} \right)^{-1}, \qquad (4.5)$$

where k_B is the Boltzmann's constant, e is the elementary charge and T is the temperature. The values of V_{OC} and τ were about constant as shown in Table 4.3 and Table 4.4, respectively.

This was suggested that the CuO-Cu$_2$O layers had almost no effect on V_{OC} and τ. Thus, both of parameters have a slight change. However, at 6 mM, the CuO-Cu$_2$O layer exhibited significant changes of R_{sh} and R_{ct}. This was probably due to two feasibility reasons.

First, Cu$_2$O has a direct band gap of ~2.1 eV, which is suitable for photovoltaic conversion, since it has high carrier concentration [131]. Whereas, CuO is a good solar spectral absorption but it is not as a good carrier as Cu$_2$O [132]. Preparation of CuO and Cu$_2$O mixed phases led to their unique physical properties consisting of both high carrier concentration and wider absorption. Thus, the mixed phases of copper oxide nanoparticles may have an advantage over pure CuO as photovoltaic devices.
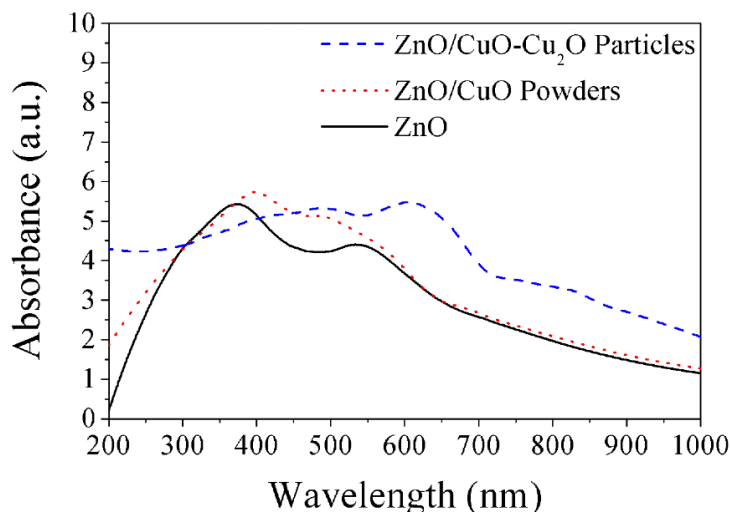
Figure 4.13. UV-vis absorption spectra of N179 dye coating on ZnO, ZnO/pure CuO (6 mM) and ZnO/CuO-Cu_2O (6 mM).

It was clearly confirmed by the UV-vis absorption spectra as shown in Figure 4.13. It was obviously that ZnO/CuO and pure ZnO layer exhibited an intrinsic absorption with intensity below 450 nm. Whereas, the ZnO/CuO-Cu_2O layer can absorb spectra in the whole wavelength region of UV-visible and can absorbed more spectra in the wavelength region of 450-1,000 nm.

Second, coated larger size of CuO-Cu_2O nanoparticles on relative smaller size of ZnO can increase carrier collection because of a light scattering increase (see Figure 4.9 (e)). The light scattering of the CuO-Cu_2O layer was measured before and after the dye sensitization by UV-vis diffused reflectance spectra as shown in Figure 4.14. The CuO-Cu_2O layer showed a strong light scattering. Especially, after dye sensitization, the CuO-Cu_2O layer exhibited the highest light scattering effect in the long wavelength range of 700-800 nm. More light scattering effected on a low R_{ct} of ZnO/CuO-Cu_2O layer at 6 mM. The result showed the minimum value R_{ct} of 13.26 Ω, which was decreased by more than 71% and 20%, compared to the pure ZnO and ZnO/CuO, respectively. This was maybe, also, due to CuO-Cu_2O layer at 6 mM gave optimum thickness (~6.9 μm).Thus, there was more light scattering and more transferred electrons from the CuO-Cu_2O layer to FTO glass.
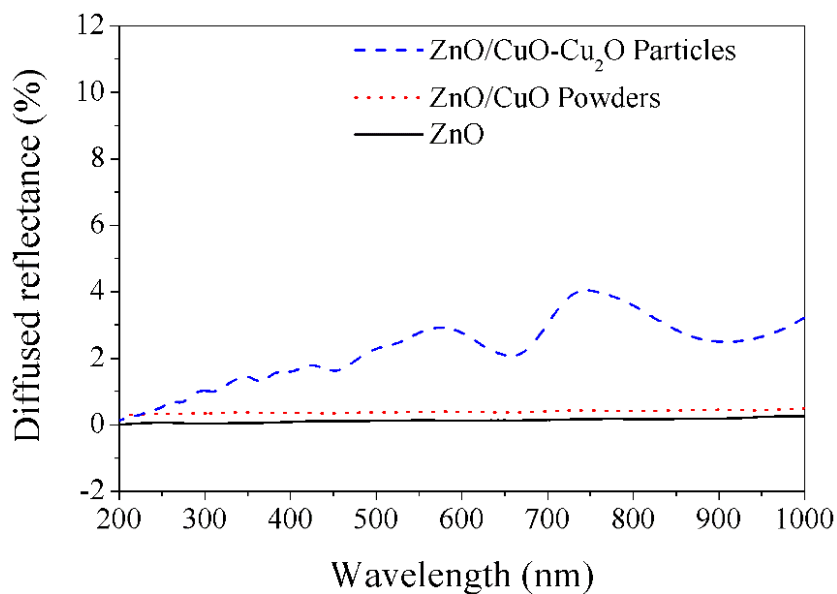
(a)
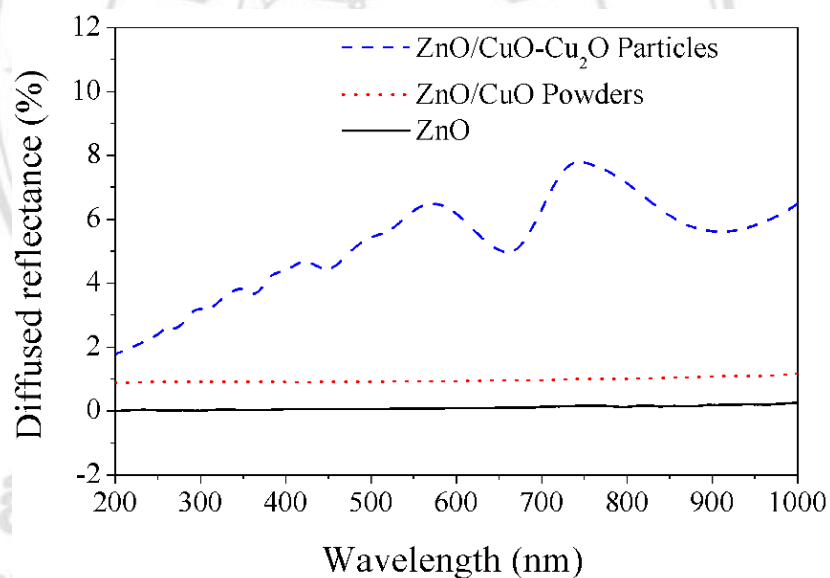
(b)

Figure 4.14 UV-vis diffused reflectance spectra of ZnO, ZnO/CuO (6 mM) and ZnO/CuO-Cu$_2$O (6 mM) (a) before and (b) after dye sensitization.

Whereas, the particle size of pure CuO (diameter < 50 nm) was not significantly different from ZnO (diameter ~30 nm). Then, pure CuO layer gave approximately less thickness than CuO-Cu$_2$O layer. This led to lower light scattering and lower charge carrier than that of the CuO - Cu$_2$O.
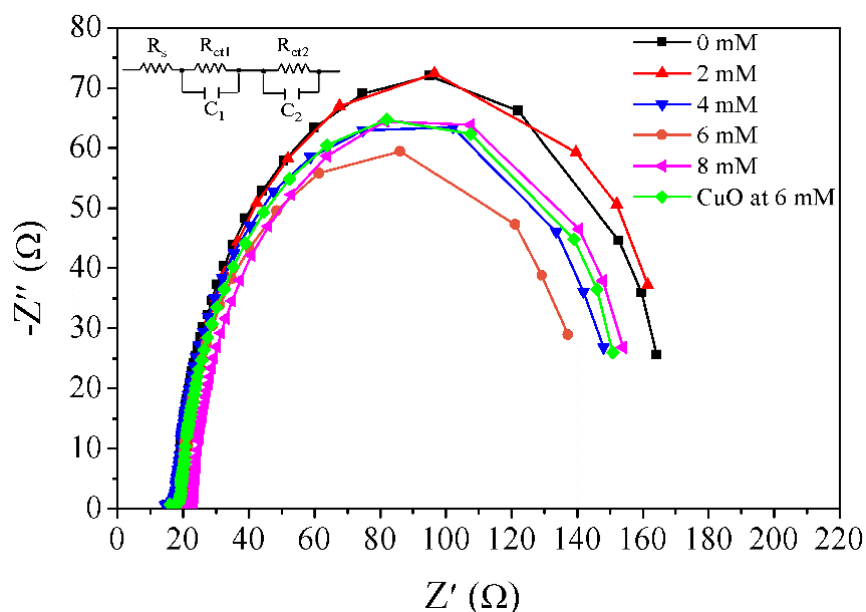
Figure 4.15. Impedance spectra of ZnO DSSCs with different concentrations of CuO-Cu$_2$O layer and pure CuO layer at 6 mM under dark condition with reward bias voltage.

As a result, pure CuO showed the lower of J_{SC} and η.

However, the coating of larger nanoparticle size led to lowering of the internal surface area of the photoelectrode film resulting in an increase of electron transport length and electron recombination [133]. This was clearly supported by a lower R_{sh} of ZnO/CuO-Cu$_2$O layer than ZnO/pure CuO. The lower R_{sh} was indicative of more opportunity in electron loss during travelling to FTO. This, also, corresponded to the EIS spectra of ZnO DSSCs with reward bias -0.75 V under dark condition as shown in Figure 4.15.

The results indicated that ZnO/CuO-Cu$_2$O at 6 mM was more sensitive to recombination than the others. Consequently, the fabrication of the CuO-Cu$_2$O nanoparticle layer on ZnO DSSCs provided higher photo current. The mixed phases of CuO-Cu$_2$O nanoparticles can expand the photon absorption range, leading to significant improved photovoltaic properties of ZnO DSSCs. Moreover, the large homogeneous size of nanoparticles increased light scattering, resulting in the highest J_{SC} and maximum η. Although,

CuO-Cu$_2$O layer at 6 mM exhibited more recombination, an extremely injected electrons from CuO-Cu$_2$O layer can, also, transferred to FTO glass as confirmed by a reduction of R_{ct} comparing to the DSSCs without CuO-Cu$_2$O and that with pure CuO layer.

4.3 Comparison between Copper Oxide Nanofibers and Nanoparticles in ZnO based DSSCs

ZnO based DSSCs with different morphologies of mixed-phase copper oxide nanostructures were employed as a double layer to improve the DSSCs efficiency.

At the same concentration, 6 mM, ZnO based DSSCs with nanofiber layer can absorb more dye than ZnO based DSSCs with nanoparticle layer but showed a lower of J_{SC} and η. ZnO based DSSCs with nanofiber layer showed the highest J_{SC} and η of 6.93 mA/cm^2 and 1.87% at V_{OC} of 0.56. Whereas, ZnO based DSSCs with nanoparticle layer represented the highest J_{SC} and η of 7.33 mA/cm^2 and 2.31% at V_{OC} of 0.65. This was suggested that electron transportation in the nanofibers may be limited by their inner structure, which resulted in the lower of J_{SC} and V_{OC}. The V_{OC} is the potential different between quasi-Fermi level electrons in copper oxide nanostructures and redox potential of the redox couple in electrolyte as shown in Figure 4.16 [134].
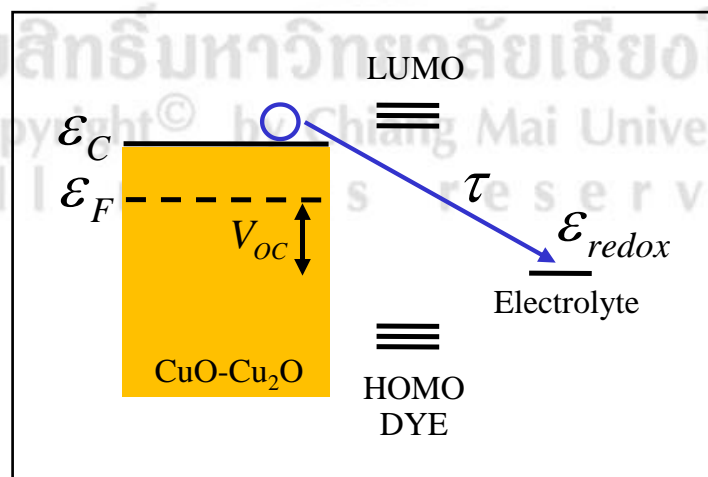

Figure 4.16. Schematic image of V_{OC} in copper oxide nanostructures in ZnO based DSSCs.

This can be written as follows : [135]

$$qV_{OC} = E_F - E_{redox},$$

(4.6)

where q is charge, E_F is the quasi-Fermi level $\left(E_F = E_C + kT \ln \dfrac{n_c}{N_C} \right)$, and E_{redox} is the electrolytic redox level. Therefore,

$$V_{OC} = \frac{kT}{q} \left(\frac{E_C - E_{redox}}{kT} + \ln \frac{n_c}{N_C} \right),$$

(4.7)

where kT is the thermal energy, n_c is the charge density in the conduction band of copper oxide and N_C is the density of accessible state in the conduction band. Thus, the V_{OC} of ZnO based DSSCs with copper oxide nanoparticles can significantly higher than the other one by 2 reasons. First, charge density in the conduction band of copper oxide nanoparticles were improved than the charges in nanofibers due to the nanoparticles are single crystal structures (from Figure 2.13). Then, the nanoparticles made easier for transportation of injected charges than the nanofibers, which were a polycrystalline (from Figure 2.7). This led to an increase of n_c and the higher of V_{OC}. Second, synthesis of copper oxide structure in nanoparticle form effected on its conduction band. According to Eq. (4.7), negative shift of a conduction band edge of the copper oxide nanoparticle responsible for an increase of V_{OC}. Both the reasons gave the higher of V_{OC}, caused an increase of J_{SC}, and resulted in the better performance of ZnO based DSSCs with copper oxide nanoparticle layer than the ZnO based DSSCs with copper oxide nanofiber layer.

4.4 Chapter Summary

Mixed phases of copper oxide CuO-Cu_2O nanofibers were prepared in viscous solution form at different masses of 1.14, 2.28, 3.42, 4.56, and 5.70 mg. Whereas, mixed phases of copper oxide CuO-Cu_2O nanoparticles were prepared in viscous solution form with various concentrations at 2, 4, 6, 8 and 10 mM. Then, both of them were coated on the ZnO photoelectrode in the DSSCs for efficiency enhancement.

For the ZnO based DSSC with CuO-Cu_2O nanofiber layer, the highest photoconversion efficiency of 1.87% and the highest current density of 6.93 mA/cm^2 were observed at a density of 3.42 mg/cm^2. The efficiency and the current density were increased by 15.4% and 26.2% over a pure ZnO layer, respectively. The increases were related to a high surface area, more dye adsorption and a wide absorption range in the optimum mixed phases of copper oxide nanofibers, leading to an increase of charge transport and a suppression of recombination. The results were confirmed by an increase of R_{sh} together with a decrease of R_s and R_{ct}.

Similarity, the DSSC with CuO-Cu_2O nanoparticle layer at 6 mM exhibited the highest performance; current density of 7.33 mA/cm^2, open circuit voltage of 0.65 V, and power conversion efficiency of 2.31%. Although the nanoparticle layer was favored both charge current and recombination, the injected electrons were improved more than electron loss in the photoelectrodes. The light-harvesting enhancement was due to larger light absorption and light scattering of the CuO-Cu_2O nanoparticle layer than that of the pure ZnO layer.

The main content of synthesis, characterization and application of mixed phases copper oxide nanostructures, CuO-Cu_2O nanofibers and CuO-Cu_2O nanoparticles, in this synthesis were summarized in the chapter 5.